Study of $Ni_{80}Fe_{20}/Fe_{50}Mn_{50}$ superlattice microstructures by transmission electron microscopy and x-ray diffraction

2001 J. Phys.: Condens. Matter 13 2891

(http://iopscience.iop.org/0953-8984/13/13/304)

INSTITUTE OF PHYSICS PUBLISHING JOURNAL OF PHYSICS: CONDENSED MATTER

J. Phys.: Condens. Matter **13** (2001) 2891–2899 www.iop.org/Journals/cm PII: S0953-8984(01)18260-3

Study of $Ni_{80}Fe_{20}/Fe_{50}Mn_{50}$ superlattice microstructures by transmission electron microscopy and x-ray diffraction

Ming Xu[1,3], Tao Yang[1], Guangming Luo[1], Zhengqi Lu[1], Cuixiu Liu[1], Ning Yang[1], Zhenhong Mai[1], Wuyan Lai[1], Zhonghua Wu[2] and Jun Wang[2]

[1] Institute of Physics, Chinese Academy of Sciences, PO Box 603-28, Beijing 100080, People's Republic of China
[2] Synchrotron Radiation Laboratory, Institute of High Energy Physics, Chinese Academy of Sciences, Beijing 100039, People's Republic of China

Received 28 September 2000, in final form 2 January 2001

Abstract

The detailed microstructures of $Ni_{80}Fe_{20}/Fe_{50}Mn_{50}$ superlattices have been characterized using both x-ray diffraction techniques and transmission electron microscopy. The obvious layered structure, typical column structure and twins which exist in $Ni_{80}Fe_{20}/Fe_{50}Mn_{50}$ superlattices were observed through performing transmission microscopy. By combining the technique of low-angle x-ray reflectivity (specular and off-specular scans) with the anomalous scattering effect and high-angle x-ray diffraction (using conventional x-ray), we quantitatively analysed the microstructural variation as a function of annealing temperature. It is found that the lateral correlation length, the (111) peak intensity of the superlattices and the average multilayer coherence length all increase with a rise in annealing temperature. The correlated roughness slightly decreases after annealing, while moderate annealing can decrease the root-mean-square roughness at the interfaces of $Ni_{80}Fe_{20}/Fe_{50}Mn_{50}$ superlattices. The obtained microstructural knowledge will be helpful in understanding the magnetic properties of the $Ni_{80}Fe_{20}/Fe_{50}Mn_{50}$ exchange bias system.

1. Introduction

Since interface exchange coupling (IEC) between ferromagnetic (FM) and antiferromagnetic (AF) layers was first observed in the 1950s [1], the FM/AF multilayers have attracted much interest in basic research [2, 3]. Theoretically, there have been two typical models [1, 4] proposed to explain the IEC phenomenon between FM and AF layers, both of which are based on the assumption of FM/AF interfacial structures. The first model, suggested by Meiklejjohn [1], supposes that the spins of the first AF layer are aligned

[3] Correspondence to Ming Xu.

ferromagnetically, resulting in an uncompensated net magnetic moment. The other model, proposed by Malozemoff [4], considers the FM/AF interface to be imperfect with the existence of random-exchange interactions between the AF and FM spins. From the point of view of microstructure, these models actually give rise to the following question: how does the interfacial structure affect the IEC? Experimentally there has also been much work to relate the IEC to the microstructures such as measurements of grain size, crystal axis distributions and interfacial structure [5–8]. It has been revealed that the *good texture* and large grain size tend to yield strong exchange coupling between the AF and FM layers. It was also found that the IEC is very sensitive to the interfacial structure, and that the interdiffusion at the AF/FM interface can produce a strong exchange bias. Contrary to this, the result of Choukh [9] indicated that a smooth and sharp interface tends to result in a homogeneous and strong enough exchange bias field. The above dissension suggests that a complete structural examination is necessary for AF/FM multilayers.

In recent years, the IEC effect has also found technological application in the form of producing an exchange-biasing field in spin-valve structures [10–12]. In the process of preparing a device, the multilayers usually undergo several cycles of thermal treatment at 100–300 °C, requiring that the multilayered structure is sufficiently stable against temperature. Although it is indispensable to perform a thermal annealing study on the microstructure of AF/FM multilayers, to date, there is no detailed knowledge of them—possibly due to the inherent difficulty in analysing quantitatively the structures of AF/FM bilayers. As is well known, in order to obtain quantitative structural information, the best way is to prepare samples in the form of superlattices. Recently, a new memory effect in ferro/antiferromagnetic multilayers was claimed, which is expected to occur also for ferro/antiferromagnetic superlattices [13]. In this work, we prepared a set of $Fe_{50}Mn_{50}/Ni_{80}Fe_{20}$ superlattices, the formation of which was examined using high-resolution cross-section TEM (transmission electron microscopy). Combining low-angle x-ray diffraction (LAXRD) with high-angle x-ray diffraction (HAXRD) measurements, the effect of annealing on the microstructure of $Fe_{50}Mn_{50}/Ni_{80}Fe_{20}$ superlattices was quantitatively analysed. The results contained in this paper will be helpful in providing a greater understanding of the magnetic properties of FeMn/NiFe multilayers.

2. Experiment

$[Ni_{80}Fe_{20}(60\ Å)/Fe_{50}Mn_{50}(50\ Å)]_{15}$ superlattices with a 60 Å Ta buffer and a 15 Å Ta cap layer were deposited on a water-cooled single-crystal silicon substrate by magnetron sputtering. All samples were prepared with a working pressure of 0.6 Pa and a base pressure of 3.5×10^{-5} Pa. Annealing was performed in a vacuum furnace with a pressure of less than 10^{-3} Pa at temperatures of 100, 200, 300 and 400 °C, respectively.

The cross-section of $[Ni_{80}Fe_{20}/Fe_{50}Mn_{50}]_{15}$ superlattices was directly observed on a Hitachi H-9000NAR high-resolution transmission microscope (HRTEM). HAXRD measurements were performed on a Rigaku diffractometer attached to a 12 kW rotating anode x-ray generator. A focusing graphite monochromator was used to obtain a high-intensity Cu Kα beam. Reflectivity measurements such as a specular reflectivity (θ–2θ) scan and a transverse scan of the first Bragg peak were carried out using the x-ray diffraction station at the Beijing Synchrotron Radiation Facility (BSRF). The incident energy was selected to be 6.5 keV. Two detector slits with a 0.2 mm wide aperture in the scattering plane were mounted on the detector arm close to the sample in order to reduce scattering between the monochromator and the sample.

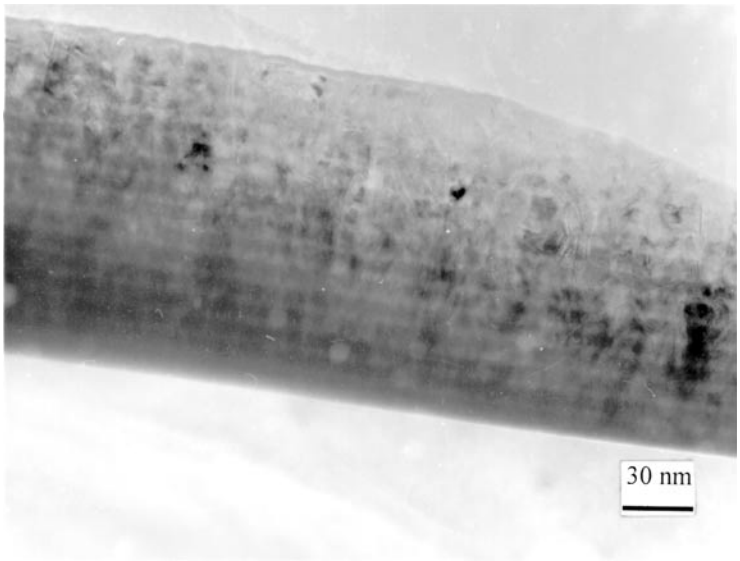

Figure 1. Cross-sectional TEM image of an as-deposited $[Ni_{80}Fe_{20}/Fe_{50}Mn_{50}]_{15}$ superlattice.

3. Results and discussion

3.1. TEM observation of $Ni_{80}Fe_{20}/Fe_{50}Mn_{50}$ multilayer structure

Figure 1 shows the cross-section TEM image of as-deposited $[Ni_{80}Fe_{20}/Fe_{50}Mn_{50}]_{15}$ superlattices from which one can see the obvious layered structures and geometrical roughness on a larger scale. The difference between bright and dark stripes, corresponding respectively to the NiFe and FeMn sublayers, is modest because of their small elemental contrast resulting from the respective electron scattering factors of Ni and Mn. The $Ni_{80}Fe_{20}$ and $Fe_{50}Mn_{50}$ sublayers are generally flat at the early stage of growth and may gradually become wavy when the film grows thick. For this reason, the surface roughness does not necessarily mean that there is a rough interface in the multilayers.

Another general feature of the $[Ni_{80}Fe_{20}/Fe_{50}Mn_{50}]_{15}$ superlattices is the columnar crystallite structure (CCs). Figure 2(a) provides a high-resolution TEM image of CCs. The marked arrows, indicate the presence of grain boundaries, or disordered structure, the lateral size of which is approximately 15 nm. From figure 2(a), it is clear that all of the CCs run across the $Ni_{80}Fe_{20}$ and $Fe_{50}Mn_{50}$ sublayers, and that the sublayers in some CCs are flat but curved or tilted in others. It can also be seen that the multilayer structure becomes undefined in the region of CCs. A possible explanation for this is that there is alternate and coherent growth of $Ni_{80}Fe_{20}$ and $Fe_{50}Mn_{50}$ in the CCs because the lattice mismatch between fcc $Ni_{80}Fe_{20}$ and fcc $Fe_{50}Mn_{50}$ is very small (about 2%). Furthermore, twin structures are observed within the CCs. Region $\boldsymbol{a}$ shows the gradual lattice transition by a slight tilting of the lattice plane. The selected area electron diffraction pattern in figure 2(b) shows that the CCs includes $Ni_{80}Fe_{20}$ and $Fe_{50}Mn_{50}$ sublayers growing preferentially along the [111] direction.

While one can directly observe the general features of the multilayers by TEM, the detailed structural information at the interfaces cannot be obtained from such measurements. For this reason, the microstructures and their change with annealing temperature were examined using low-angle x-ray diffraction (LAXRD) and high-angle x-ray diffraction (HAXRD) measurements.

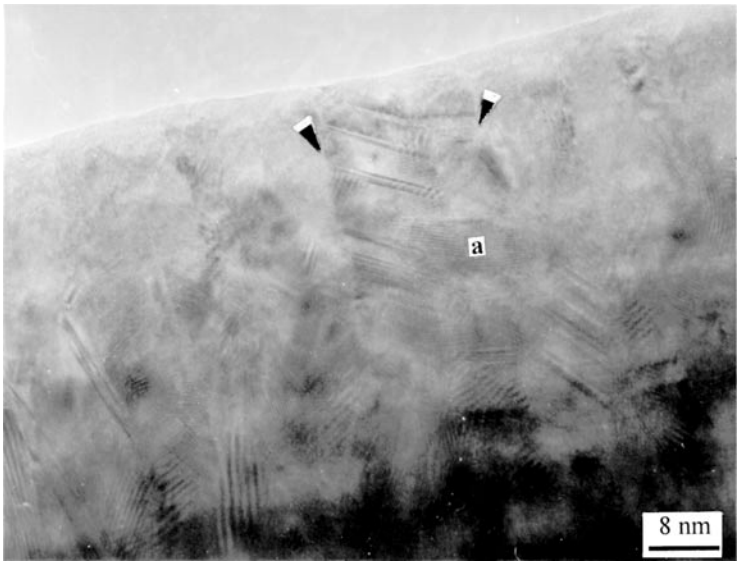

(a)

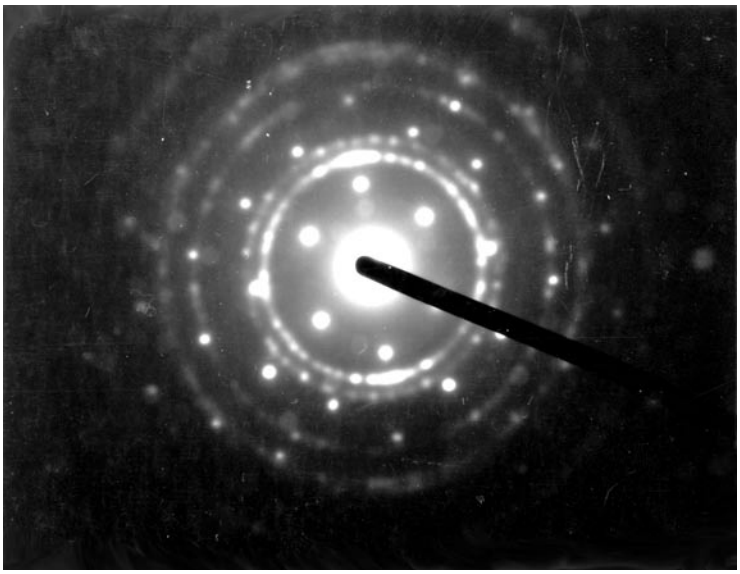

(b)

Figure 2. (a) HRTEM image of a columnar crystallite in $[Ni_{80}Fe_{20}/Fe_{50}Mn_{50}]_{15}$ superlattices. (b) Selected area electron diffraction pattern of the columnar crystallite.

3.2. Characterization of $Ni_{80}Fe_{20}/Fe_{50}Mn_{50}$ multilayer structure by XRD

3.2.1. Low-angle x-ray diffraction. As is well known, a small x-ray contrast between $Ni_{80}Fe_{20}$ and $Fe_{50}Mn_{50}$ for Cu Kα radiation exists by virtue of the proximity of the atomic numbers for Ni, Fe and Mn in the periodic table. In general, the incident x-ray energy slightly lower than the absorption edge of lighter elements is expected to greatly enhance the Bragg peak intensity [14]. Therefore, in order to increase both the numbers of observed Bragg peaks and the

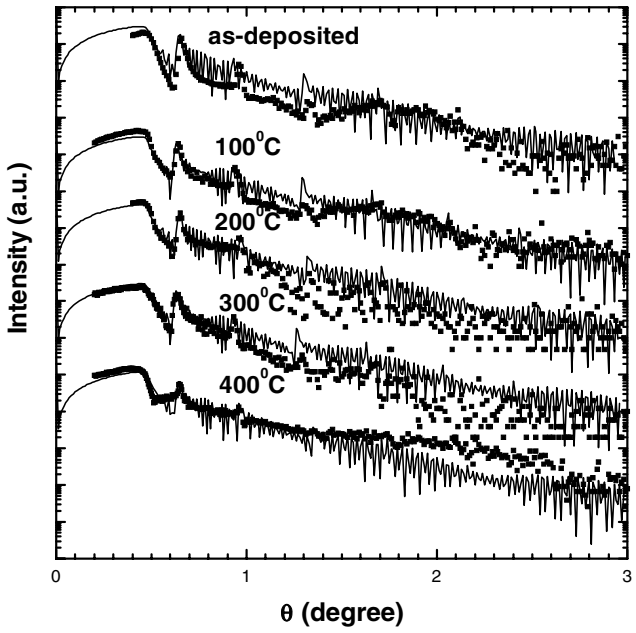

Figure 3. Low-angle x-ray diffraction patterns of $[Ni_{80}Fe_{20}/Fe_{50}Mn_{50}]_{15}$ superlattices for different annealing temperatures. The squares and solid lines correspond to experimental and simulated results, respectively.

Table 1. Structural parameters of $Ni_{80}Fe_{20}/Fe_{50}Mn_{50}$ superlattices obtained from x-ray reflectivity and diffuse scattering.

Annealing condition	I_1	I_2	t_{NiFe} (Å)	t_{FeMn} (Å)	σ (Å)	σ_{cor} (Å)	ξ (Å)	h
As-deposited	898	178	73	56	4 ± 1	2 ± 0.2	200 ± 50	0.8–1
100 °C	736	274	77	60	3 ± 1	2 ± 0.2	500 ± 50	0.8–1
200 °C	729	185	75	54	3.5 ± 1	1.8 ± 0.2	1200 ± 200	0.8–1
300 °C	734	182	77	60	3 ± 1	1.5 ± 0.2	5000 ± 500	0.8–1
400 °C	640	99	75	55	5 ± 1	1.5 ± 0.2	5000 ± 500	0.8–1

diffraction intensity, the incident x-ray energy near to the Mn absorption edges (6.5 keV) was tuned using the synchrotron radiation source at BSRF. Figure 3 shows the LAXRD patterns of the $Ni_{80}Fe_{20}/Fe_{50}Mn_{50}$ multilayers. Clearly visible in each curve are three superlattice peaks, indicating a high-quality periodic structure for the $Ni_{80}Fe_{20}/Fe_{50}Mn_{50}$ multilayers—consistent with the result of our TEM observation. If the multilayers are not highly crystalline and have only a moderate number of periods, the interfacial roughness can be estimated from the intensities of low-angle diffraction peaks [15]. In table 1, we list the intensities of the first (I_1) and second (I_2) peaks, from the variation of which one can infer that moderate annealing may improve the interface structure.

Since the LAXRD is sensitive to the chemical compositions of each sublayer in the multilayers, one can obtain the interfacial information from the LAXRD profiles of the multilayers. By theoretically simulating (the method for which one can obtain from [16]) the LAXRD profiles (the solid curves in figure 3), the interfacial rms (root-mean-square) roughnesses (σ) of the superlattices were obtained. The simulated results are listed in table 1,

from which one can see that σ decreases with increasing annealing temperature, until a critical point at 400 °C where σ begins to increase.

Figure 4 shows the transverse scans of the $Ni_{80}Fe_{20}/Fe_{50}Mn_{50}$ multilayers with the detector angle fixed at the first Bragg peak position. As is well known, the geometrical component of the roughness at the surface and/or interface induces diffuse scattering while intermixing at the interface produces no diffusive scattering, only inducing electron density changes in the normal direction. The weak diffuse scattering evident in figure 4 indicates that there is a small geometrical roughness in the $Ni_{80}Fe_{20}/Fe_{50}Mn_{50}$ multilayers. Structural parameters such as the correlated roughness (σ_{cor}), lateral correlation length (ξ) and fractal parameter (h) were obtained by simulating the experimental results, as shown in table 1. These parameters have been defined elsewhere [16]. There is not much change in the fractal parameter (h) that reflects the geometrical fluctuation at the interface during annealing. h is close to 1, indicating that the interface between $Ni_{80}Fe_{20}$ and $Fe_{50}Mn_{50}$ layers is smooth. The lateral correlation length increases with increasing annealing temperature, meaning that the interface in $Ni_{80}Fe_{20}/Fe_{50}Mn_{50}$ multilayers becomes smoother with rising temperature. Furthermore, the parameters listed in table 1 indicate that the correlated roughness is small, and only slightly decreases with an increase in annealing temperature.

The above changes of the interfacial microstructure may be due to the simultaneous atomic diffusion at interfaces and grain boundaries. When the $Ni_{80}Fe_{20}/Fe_{50}Mn_{50}$ multilayers are annealed at low temperature (i.e. below a critical temperature), the atomic diffusion at the interfaces occurs inside each grain. This process will be helpful to improve the interfacial state. At a higher annealing temperature (i.e. over a critical temperature), the atomic diffusion at grain boundaries causes the layers to undulate, and the diffusion at interfaces leads to more diffuse interfaces. In the $Fe_{50}Mn_{50}/Ni_{80}Fe_{20}$ system, since the original interface is enriched in Ni, the substantial Ni content would diffuse into the $Fe_{50}Mn_{50}$ sublayers close to the interface

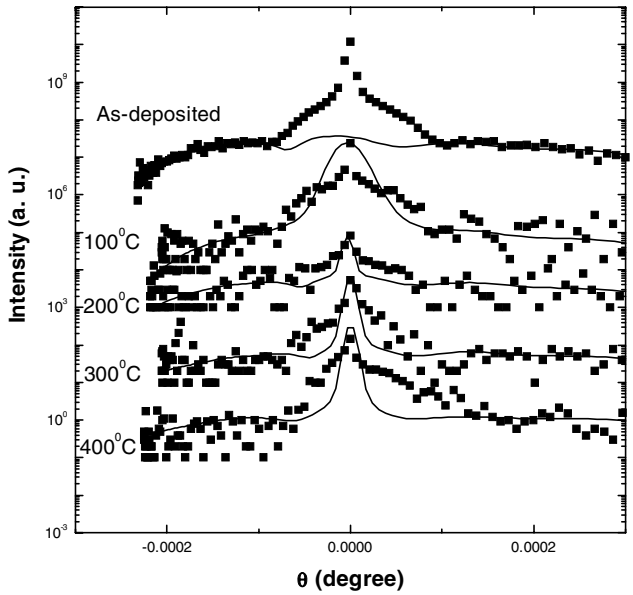

Figure 4. Transverse diffuse scans through the first Bragg peak of $[Ni_{80}Fe_{20}/Fe_{50}Mn_{50}]_{15}$ superlattices for different annealing temperatures. The squares and solid lines correspond to experimental and simulated results respectively.

after annealing at the higher temperature. This phenomenon has been demonstrated by Auger composition analysis [17]. On the other hand, there is also grain boundary motion for the $Ni_{80}Fe_{20}$ grain as suggested by Cook and Hilliard [18]. The moving interfaces can provide high-diffusivity paths. The atomic diffusion along the grain boundary may favour decreasing the whole geometrical fluctuation, so that, in turn, the correlated roughness decreases with an increase in annealing temperature.

3.2.2. High-angle x-ray diffraction. Figure 5 shows the high-angle x-ray diffraction patterns of the $Ni_{80}Fe_{20}/Fe_{50}Mn_{50}$ multilayers. The solid square symbol corresponds to the experimental results. Only the (111) peaks can be seen clearly (at about 43.5–44°) in the HAXRD patterns, respectively. This is because the peaks of the $Ni_{80}Fe_{20}$ and $Fe_{50}Mn_{50}$ sublayers are superimposed with a small lattice mismatch in fcc structure. From figure 5, one can see that as the annealing temperature increases, the intensity of the (111) peak increases, also indicating an increase of the [111] preferred orientation. It is interesting to note that, as the annealing temperature increases, the diffraction peak slightly shifts to the low-angle direction. This means that the average interplane distance, $\overline{d}$, of $Ni_{80}Fe_{20}/Fe_{50}Mn_{50}$ multilayers increases slightly. The values for $\overline{d}$ as calculated from the diffraction peak positions are given in table 2.

From the zero-order peak of the HAXRD, one can further determine the average coherence length, L_M, according to [19]:

$$L_M = M\Lambda/(1 + M\Lambda\Gamma\cos\theta/\lambda)$$

where M is the number of bilayers, Λ the superlattice period, Γ the host (111) peak broadening in radians, $\cos\theta$ is generally approximated by $[1-(\lambda/2\overline{d})^2]^{1/2}$, where λ is the x-ray wavelength, and $\overline{d}$ is the average interplane distance. The values of L_M calculated for the (111) peaks are listed in table 2. One can see that the average coherence length of $Ni_{80}Fe_{20}/Fe_{50}Mn_{50}$

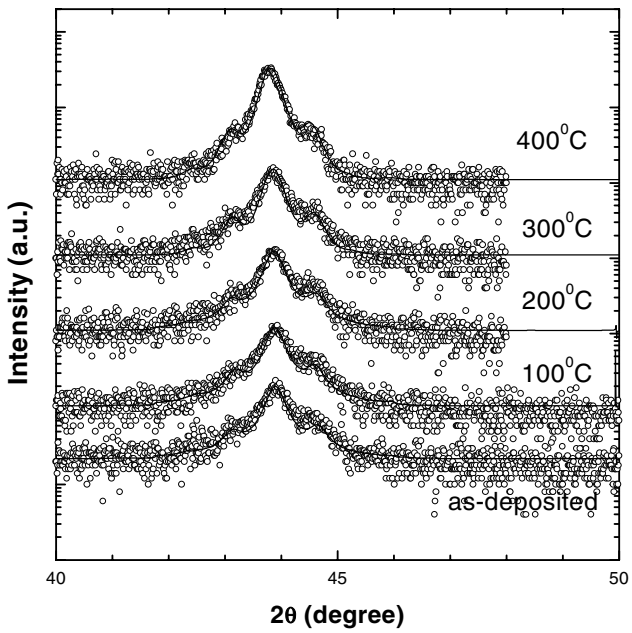

Figure 5. High-angle x-ray diffraction (open circles) and computer simulations (solid lines) for $[Ni_{80}Fe_{20}/Fe_{50}Mn_{50}]_{15}$ superlattices.

Table 2. Structural parameters of $Ni_{80}Fe_{20}/Fe_{50}Mn_{50}$ superlattices obtained from high-angle x-ray diffraction. A and B correspond to $Ni_{80}Fe_{20}$ and $Fe_{50}Mn_{50}$, respectively.

Annealing condition	L (Å)	d (Å)	d_{NiFe} (Å)	d_{FeMn} (Å)	N_A	N_B	$N_{A/B}$	$N_{B/A}$
As-deposited	254.3	2.060	2.045	2.084	36	25	0	0
100 °C	283.0	2.060	2.045	2.084	38	27	0	0
200 °C	280.6	2.061	2.047	2.084	36	25	0	0
300 °C	338.2	2.063	2.046	2.084	35	29	0	0
400 °C	382.4	2.065	2.05	2.084	37	28	0	0

multilayers is approximately 255–383 Å—much smaller than the size of the CCs determined from TEM. This is because x-ray diffraction gives an average result. Furthermore, from table 2, one can see that the value of L_M increases with increasing annealing temperature. To some extent, this demonstrates a structural improvement of the $Ni_{80}Fe_{20}/Fe_{50}Mn_{50}$ multilayers during annealing. It was believed that an epitaxial ferromagnetic/antiferromagnetic multilayer system could result in an increase of the exchange anisotropy energy [20]. Therefore moderate annealing would be helpful to exchange bias.

The solid curves in figure 5 are theoretical simulations of the HAXRD profiles for the $Ni_{80}Fe_{20}/Fe_{50}Mn_{50}$ multilayers, assuming a linear-interface model [21]. This model has proven valid for analysing the polycrystalline superlattice structure [21, 22]. By fitting the positions of the main peak and the satellites, the structural parameters, such as the atomic plane number of each sublayer N_{NiFe}, N_{FeMn}, $N_{NiFe/FeMn}$ and $N_{FeMn/NiFe}$, the interplanar distances of the $Ni_{80}Fe_{20}$ and $Fe_{50}Mn_{50}$ layers, d_{NiFe} and d_{FeMn}, can be obtained (seen in table 2). The values of d_{NiFe} (of the order of 2.045–2.05 Å) and d_{FeMn} (2.084 Å) strongly suggest that both $Ni_{80}Fe_{20}$ and $Fe_{50}Mn_{50}$ layers grow preferentially along the [111] direction. One can see from table 2 that d_{NiFe} increases slightly as the annealing temperature increases, indicating that the $Ni_{80}Fe_{20}$ sublayers were slightly relaxed after annealing. Furthermore it is noted that, both before and after annealing, there is no intermixing interface between the $Ni_{80}Fe_{20}$ and $Fe_{50}Mn_{50}$ sublayers—in contrast to $Ni_{80}Fe_{20}$/Mo [22] and/or $Ni_{80}Fe_{20}$/Cu [23] multilayers. This result can be attributed to the deposition of the stable γ(fcc) phase of FeMn onto fcc Permalloy [3, 8]. Since the lattice constant of γ(fcc)-$Fe_{50}Mn_{50}$ is slightly larger than that of $Ni_{80}Fe_{20}$, it is possible that the lattice constant of $Ni_{80}Fe_{20}$ in $Ni_{80}Fe_{20}/Fe_{50}Mn_{50}$ multilayers slightly increases during annealing. On the other hand, the stable γ(fcc) phase of FeMn may restrain atomic interdiffusion at the $Ni_{80}Fe_{20}/Fe_{50}Mn_{50}$ interfaces meaning that if the annealing temperature is not very high, it is reasonable for there to be no intermixing interface between the $Ni_{80}Fe_{20}$ and $Fe_{50}Mn_{50}$ sublayers. Comparing the result with that of LAXRD, we further demonstrate the possibility of atomic diffusion along the grain boundary.

4. Conclusions

The microstructures of $Ni_{80}Fe_{20}/Fe_{50}Mn_{50}$ superlattices were investigated using x-ray diffraction techniques and TEM. The characteristics such as obvious layered structure, typical column structure and crystalline twins are observed in $Ni_{80}Fe_{20}/Fe_{50}Mn_{50}$ superlattices. As the annealing temperature increases, interplanar distance, average multilayer coherence length and (111) peak intensity of the superlattices all increase while the rms interfacial roughness initially decreases before increasing for higher annealing temperatures. X-ray diffuse scattering revealed that there is significant interface correlation in $Ni_{80}Fe_{20}/Fe_{50}Mn_{50}$ superlattices with the lateral correlation length increasing with an increase of annealing temperature, and the

correlated roughness slightly decreasing after annealing. In contrast to $Ni_{80}Fe_{20}$/Mo and/or $Ni_{80}Fe_{20}$/Cu superlattices, we revealed that there is no intermixing layer between the $Ni_{80}Fe_{20}$ and $Fe_{50}Mn_{50}$ sublayers in $Ni_{80}Fe_{20}/Fe_{50}Mn_{50}$ superlattices. Since the interfacial structures significantly affect the exchange bias, the above microstructural knowledge will be helpful in understanding the magnetic properties of the $Ni_{80}Fe_{20}/Fe_{50}Mn_{50}$ system.

Acknowledgments

The authors would like to acknowledge the support of BSRF. This project was also supported by the National Natural Science Foundation of China and the Chinese Academy of Sciences.

References

[1] Meiklejjohn W P and Bean C P 1956 *Phys. Rev.* **102** 1413
Meiklejjohn W P and Bean C P 1957 *Phys. Rev.* **105** 904
[2] Meiklejjohn W P 1962 *J. Appl. Phys.* **33** 1328
[3] Hempstead R D, Krongelb S and Thompson D A 1978 *IEEE Trans. Magn.* **14** 521
[4] Malozemoff A P 1987 *Phys. Rev.* B **35** 3679
Malozemoff A P 1988 *Phys. Rev.* B **37** 7673
[5] Choe G and Gupta S 1997 *Appl. Phys. Lett.* **70** 1766
[6] Konoto M, Tsunoda M and Takahashi M 1999 *J. Appl. Phys.* **85** 4925
[7] Nishioka K, Hou C, Fujiwara H and Metzger R D 1996 *J. Appl. Phys.* **80** 4528
[8] Tsang C, Heiman N and Lee K 1981 *J. Appl. Phys.* **52** 2471
[9] Choukh A M 1997 *IEEE Trans. Magn.* **33** 3676
[10] Dieny B, Speriosu V S, Parkin S S P, Gurney B A, Wilhoit D R and Mauri D 1991 *Phys. Rev.* B **43** 1297
[11] Tsang C 1989 *IEEE Trans. Magn.* **25** 3692
[12] Lin T, Tsang C, Fontana R E and Howard J K 1995 *IEEE Trans. Magn.* **31** 2585
[13] Komada R H, Edelstein A S, Lubitz P and Sieber H 2000 *J. Appl. Phys.* **87** 5067
[14] Nakayama N, Moritani I, Shinjo T, Fujii Y and Sasaki S 1988 *J. Phys. F: Met. Phys.* **18** 429
[15] Gu Y S 1992 *PhD Thesis* University of Illinois at Urbana-Champaign and references therein
[16] Luo G M, Jiang H W, Wu F, Yan M L, Mai Z H, Lai W Y, Dong C and Wang Y T 1999 *J. Phys.: Condens. Matter* **11** 945
[17] Toney M F, Tsang C and Howard J K 1991 *J. Appl. Phys.* **70** 6227
[18] Cook H E and Hilliard J E 1969 *J. Appl. Phys.* **40** 2191
[19] Stearns M B 1988 *Phys. Rev.* B **38** 8109
[20] Speriosu V S, Herman D A Jr, Sanders I L and Yogi T 1990 *IBM J. Res. Dev.* **34** 884
[21] Stearns M B, Lee C H and Groy T L 1989 *Phys. Rev.* B **40** 8256
[22] Luo G M, Yan M L, Mai Z H, Lai W Y and Wang Y T 1997 *Phys. Rev.* B **56** 3290
[23] Xu M, Luo G M, Chai C L, Mai Z H, Lai W Y, Wu Z H and Wang D W 2000 *J. Cryst. Growth* **212** 291